

Spike detection using neural networks

Agnibho Chattarji

4th Year Project Report
Computer Science
School of Informatics
University of Edinburgh

2019

Abstract

The action potential or spike is a fundamental unit of information processing in the nervous system. Thus, understanding the neural code embedded in the spatio-temporal patterns of spiking requires powerful electrophysiological recording techniques and the appropriate quantitative tools to analyse data gathered from them. Rapid advances in Multi-Electrode Arrays (MEAs) have given rise to large volumes of high-resolution spiking data from multiple neurons at the same time. The analysis of such large-scale data requires efficient and robust algorithms for spike sorting, which includes detection of spikes, followed by their spatial localization with respect to the neurons they originated from. In this study we applied a neural network detection method to carry out efficient spike detection from biophysically-realistic simulated MEA data. To this end, we used a relatively simple Multi-Layer Perceptron (MLP) consisting of only two hidden layers to test its robustness in detecting spikes in data containing both low and high levels of background noise. We also experimented with the parameters of the neural network and assessed changes in performance. Further, we evaluated variations in performance caused by changes in the data format. Based on this work, we have established a new technique to split Hierarchical Data Format(HDF5) data to improve spike detection performance. Importantly, our model achieved high levels of accuracy in detecting spikes in the low-noise dataset without requiring any time-consuming manual interventions and without compromising on speed. In contrast, we observed reduced performance in the higher noise dataset. Despite this, in terms of reliable and accurate spike detection, the primary goal of the present study, our model was able to perform well even with the high-noise dataset. The decrease in performance with the high-noise data was seen in the domain of spike sorting, specifically assigning a detected spike to the correct channel. In summary, unlike commonly used spike-sorting algorithms that utilise separate steps for spike detection, feature extraction and clustering, in this project the entire process is considered as a whole. This model directly processed the raw input voltage signal to predict the timings of the sorted spikes. These findings raise the possibility of new ways to design more robust and scalable neural network methods for efficient and accurate detection and sorting of spiking data.

Acknowledgements

I would like to express my deepest gratitude to Prof. Matthias Hennig for his helpful guidance and support over the past year when this project was carried out under his supervision. I have learned a lot from him and his colleagues in the lab. Whatever has been achieved in this project has been possible because of his generous advice and patience. I am also very grateful to Cole Hurwitz for his advice and the many helpful discussions during this project.

Table of Contents

1	Introduction	6
2	Background	8
2.1	The action potential	8
2.2	Recording action potentials	9
2.3	Spike Coding	10
2.4	Recordings from large populations of neurons using high-density multi-electrode arrays	11
2.5	Challenges facing spike detection and sorting	12
2.6	Earlier efforts in developing spike sorting toolkits	12
2.6.1	Threshold based strategies	12
2.6.2	Template based strategies:	13
2.7	Neural networks applications in spike sorting	13
2.8	Data used in this project	14
3	Methodology	15
3.1	Pre-processing	15
3.2	Baseline Classifier	15
3.3	Creating the neural network	16
3.4	Creating the training set	16
3.5	Creating the testing set	17
3.5.1	Centring data around local minimum	17
3.6	Evaluation of model predictions	19
4	Results	20
4.1	Spike detection and sorting on low-noise dataset	20
4.2	Spike detection and sorting on high-noise dataset	22
4.3	Effect of snippet length on model performance	24
4.4	Adding neurons and a hidden layer to the model	25
4.5	Asymmetric snippets	26
5	Discussion	28
5.1	Key findings	28
5.2	Future directions	29
	Bibliography	31

Chapter 1

Introduction

The nervous system is made up of intricate networks and circuits of neurons that together give rise to an amazingly complex repertoire of behaviors, such as sensory perception, motor action, cognition and emotion. At the heart of all such neural activity lies the remarkable ability of neurons to generate and rapidly propagate electrical signals over large distances across the nervous system. Neurons carry out such signaling by generating action potentials or, spikes. Indeed, it is the specific sequences and temporal patterns of spikes fired and transmitted by neurons that together encode information in the nervous system. Ever since Hodgkin and Huxley's pioneering research (Hodgkin and Huxley [1952]) on the ionic basis of action potentials, electrophysiological recordings of spikes have occupied a central place in both experimental and theoretical analysis of how spikes represent and encode information in the nervous system. While earlier electrophysiological studies relied primarily on single-electrode in vitro or in vivo recordings, often in simpler invertebrate nervous systems, the past several decades have witnessed rapid technical developments that represent a paradigm shift. In particular, there has been explosive growth in the development and use of Multi-Electrode Arrays (MEAs) that now enable neuroscientists to record simultaneously from a large number of neurons in a variety of different neural tissues, including both in vitro preparations and in vivo recordings in awake behaving animals (Hilgen et al. [2017], Stevenson and Kording [2011], J. Jun et al. [2017]). This, in turn, has given rise to an almost exponential rise in large volumes of spiking data. Consequently, a major challenge now is to develop robust, efficient, accurate and scalable methods for detecting and sorting spikes that can make optimal use of the rapid growth of large-scale electrophysiological data (Lewicki [1998], Muthmann et al. [2015], Rey et al. [2015]).

The present study addresses certain aspects of this bigger problem by testing the efficacy of a neural network detection method to carry out efficient spike detection from biophysically-realistic simulated MEA data containing both low and high levels of background noise.

In view of the challenges and opportunities arising from these new developments at the interface of experimental and computational neuroscience, the objectives of this project are as follows:

- Develop and apply a neural network method for efficient detection of spikes from biophysically-realistic simulated MEA data containing both low and high levels of background noise, hence testing the robustness of the algorithms.
- Experiment with the parameters of the neural network and observe changes in performance.
- Experiment with the data format and observe changes in performance.

The contributions I have made to this project are briefly summarised below in the form of the following results:

- Train a Multi-Layer Perceptron(MLP) to tackle the task of spike detection.
- Created a new technique to split HDF5 data to improve spike detection performance of my model.
- Experiment with different parameters and data formats, and analyse resulting changes in model performance.

Chapter 2

Background

2.1 The action potential

The nervous system consists of cells or neurons that are specialized for generating electrical signals in response to a range of stimuli, and transmitting them to other neurons. Neurons possess two important morphological specializations - dendrites and axons (Figure 2.1). Dendrites enable neurons to receive inputs from other neurons, while the axon is the output end of the neuron through which information is sent to other neurons. The contact point between the axon and dendrite - the junction where electrical signals are passed from one neuron to the next - is called the synapse. When a neuron is sufficiently excited by the synaptic inputs impinging on it, its membrane potential gets depolarized to cross an all-or-none threshold level, and this leads to the generation of an action potential, or spike. The action potential represents an approximately 100 μV deflection in electrical potential that lasts for roughly 1 millisecond (Figure 2.2). It is this action potential or spike that travels down the axon and triggers synaptic transmission on other neurons. Further, a neuron's capacity to generate a spike is also dependent on its recent history of activity. For instance, for a few milliseconds immediately after a spike has been fired, it is impossible for the neuron to generate another action potential. This is known as the absolute refractory period (Figure 2.2). This is followed by another period that can be longer - called the relative refractory period - during which a neuron can fire a spike only with sufficient excitation. Finally, action potentials constitute a vital currency of communication because they can propagate over long distances across networks of neurons. Unlike sub-threshold membrane potentials that undergo rapid attenuation within distances of a millimetre or less, spikes undergo active regeneration as they travel along axons, and hence have the capacity to propagate rapidly over longer distances without suffering significant decay. For all of these reasons, the spike is a fundamental unit of information processing between neurons.

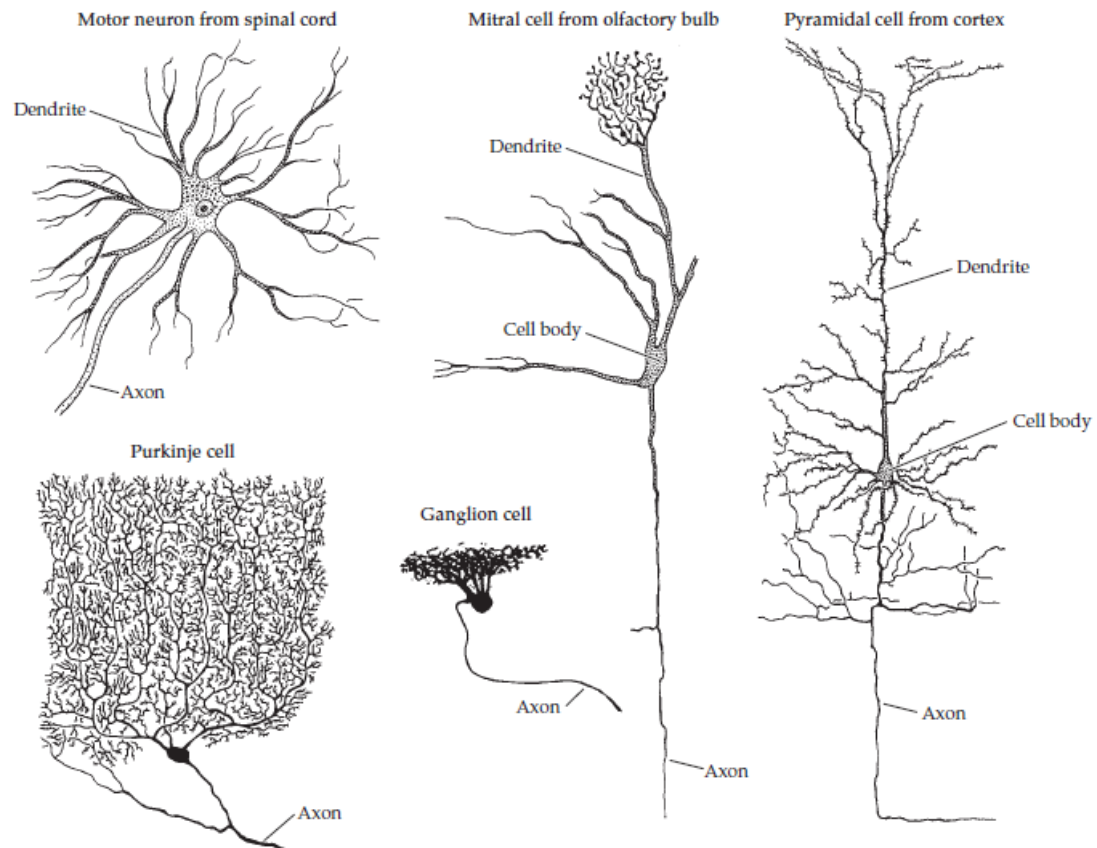


Figure 2.1: Neurons, which exhibit a wide range of shapes and sizes, have branches (called dendrites), on which other neurons form synapses, and axons that, in turn, make connections with other neurons. (Nicholls and Weisblat [2011])

2.2 Recording action potentials

Action potentials can be monitored using both intracellular and extracellular recording techniques (Figure 2.3). Typically, single-cell intracellular measurements are made using a glass electrode (either sharp or patch electrode) that is filled with a conducting electrolyte. In contrast, extracellular recordings are made by placing an electrode near a neuron without penetrating the neuron's cell membrane. Both rapid spikes, as well as underlying subthreshold potentials, can be monitored with intracellular recordings. By contrast, only spike firings can be recorded using extracellular techniques. However, *in vivo* extracellular recordings offer a powerful method for analysing spiking patterns in awake, behaving animals. Finally, as described in the next section, multi-electrode arrays also provide a powerful tool for simultaneously monitoring spiking activities from a larger number of neurons in a range of invertebrate and mammalian nervous systems.

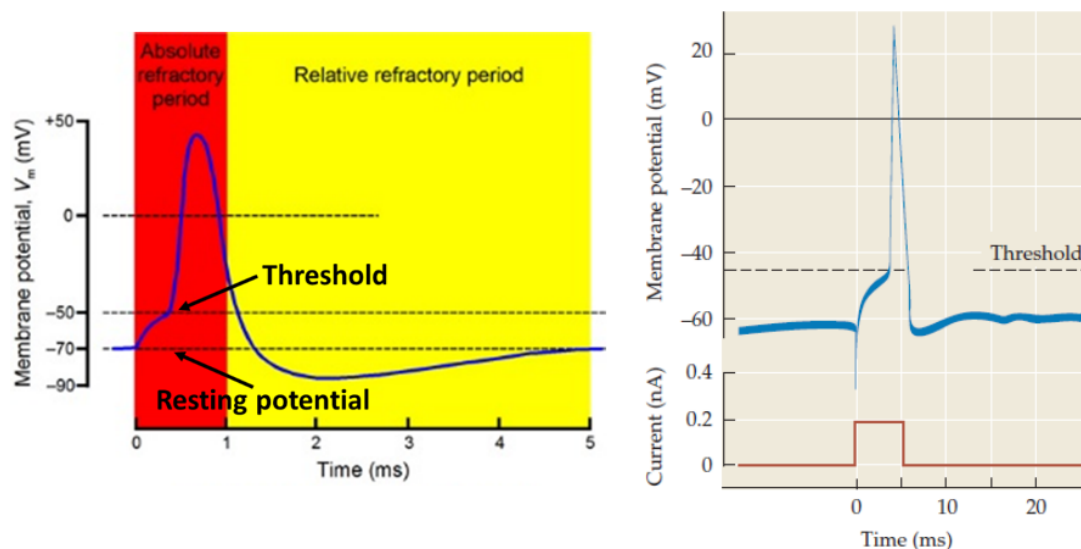


Figure 2.2: **Left:** Schematic diagram of an action potential and refractory periods (from PhysiologyWeb [2019]). Dotted lines indicate threshold for action potential generation as well as resting potential. **Right:** A real action potential recorded from a retinal ganglion cell with an intracellular micro electrode. A depolarizing current is injected (bottom red trace) into the cell through the micro electrode. This elicits a depolarizing response that crosses the spike firing threshold, which in turn leads to an all-or-nothing action potential. This spike then propagates down the axon to reach its terminal, where neurotransmitters are released at the synapse (Adapted from Nicholls and Weisblat [2011]).

2.3 Spike Coding

How neurons encode information using spikes has been of considerable interest for both experimental and computational neuroscientists. Indeed, the nature and significance of the neural code, embedded in the sequence of spikes fired by ensembles of neurons, has been a subject of long-standing discussion. Specifically, whether neurons utilize temporal or rate coding has been at the centre of these debates. The basic idea of temporal coding is rooted in the idea that the precise timing of when a spike occurs is an essential element of the information encoded in the neural response. A growing body of experimental evidence has revealed that this temporal resolution is in the order of milliseconds, thereby highlighting the fact that the precise timing of spikes is a critical feature of temporal coding. On the other hand, in rate coding, information is carried in the average rate of spikes fired by neurons. While the debate between rate versus temporal coding is not of any direct relevance to the present study, it highlights the importance of reliably detecting action potentials, and characterizing their firing patterns, in understanding their significance for neural coding.

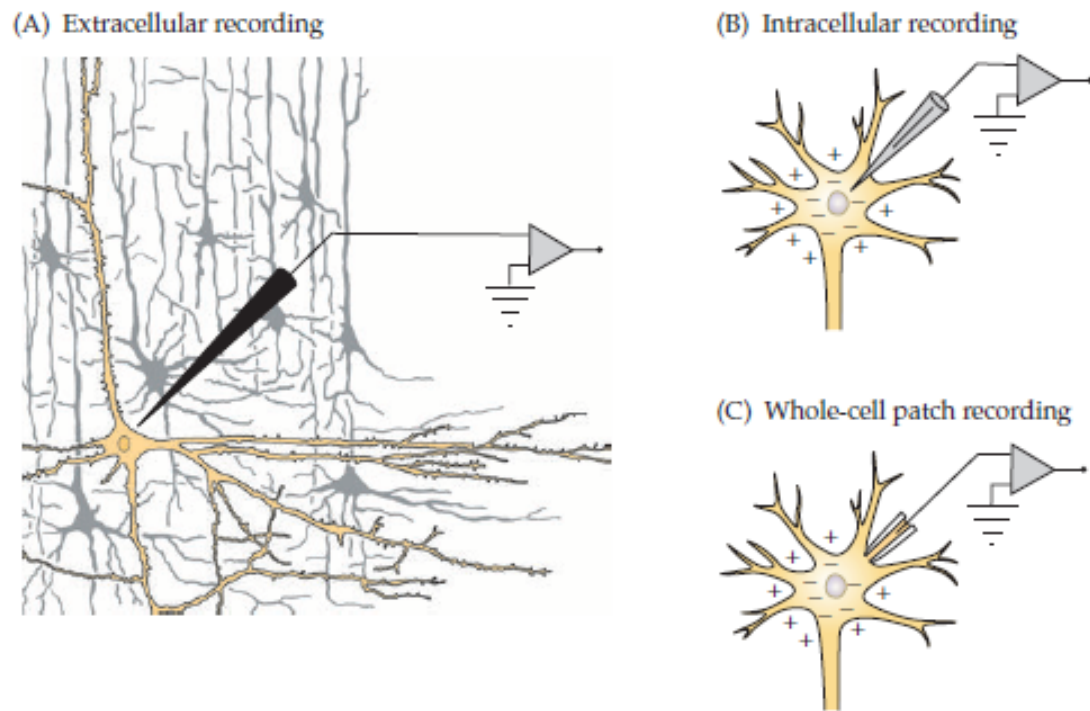


Figure 2.3: Left: Different electrophysiological recording methods. (A) Extracellular recordings can be carried out using fine wire electrodes near neurons. This enables one to record from a single neuron or from an ensemble of neurons either in vitro or in vivo. (B) Intracellular recordings, on the other hand, are obtained using fluid-filled glass electrodes that are inserted into neurons. (C) Finally, intracellular single-neuron recordings can also be made using patch electrodes. These have a larger tip diameter than that of an intracellular microelectrode. (Adapted from (Nicholls and Weisblat [2011])

2.4 Recordings from large populations of neurons using high-density multi-electrode arrays

Accumulating experimental evidence from a series of recent studies have highlighted the utility of high-density microelectrode arrays (MEAs) that offer new ways of extracellularly monitoring the firing of spikes from thousands of neurons in parallel. These MEA recordings are transformative as they represent a paradigm shift from traditional techniques that only allowed for recordings from one neuron at a time to the simultaneous sampling of neuronal activity, and its dynamics, across circuits and networks of neurons. However, gaining meaningful insights from the large volumes of raw data generated from such recordings is faced with several challenges.

2.5 Challenges facing spike detection and sorting

In addition to the obvious challenges posed by the large amounts of electrophysiological data, effective detection and analysis of MEA recordings of neural activity is associated with several basic problems. For instance, experimental recordings of extracellular waveforms exhibit varying levels of background noise that can arise either from noise in the recording amplifier, or it could reflect the neurobiological properties of the neural system under study, such as smaller spikes from neurons in the neighbourhood of the recordings. In other words, a fundamental challenge is the unambiguous classification of neuronal activity in the presence of background noise. In other words, spikes are recorded with a background of noisy activity and are typically detected, for example, by setting an amplitude threshold. However, when this threshold level is set too low, noise fluctuations may give rise to false positive events; on the other hand, if the threshold is set too high, low-amplitude action potentials are likely to be missed. Sometimes spike sorting strategies have to be applied to activities of neurons that are physically close to each other such that their firing may be picked up by the same recording electrode. Depending on the neural system being analysed, spikes being fired by two different nearby neurons may not necessarily mean that they are reflecting the same functional output. One can imagine a scenario wherein these neighbouring neurons are firings in response to different stimuli, and hence it might be necessary to dissect which spike corresponds to which neuron. Yet another layer of complexity arises from the challenge of detecting and classifying multiple spike shapes simultaneously. Finally, another challenge is posed by the classification of spikes that overlap in time. Interestingly, relevant to the present study, one of the approaches to the problem of temporally overlapping spikes has been to use neural networks (Jansen [1990], Chandra and Optican [1997]). For example, (Chandra and Optican [1997]) have shown that a trained neural network is capable of performing as well as a matched-filter strategy for classifying non-overlapping action.

2.6 Earlier efforts in developing spike sorting toolkits

In light of the various challenges described in the previous section, the development of efficient and robust toolkits for spike sorting have relied on a range of strategies. While a detailed review of these methods is beyond the scope of this report, spike sorting toolkits utilize two basic steps (a) the detection of spiking events from electrophysiological data, and (b) the attribution of each of the detected events to a specific neuron, a process known as sorting. Earlier research aimed at designing such strategies broadly fall into two categories:

2.6.1 Threshold based strategies

As discussed earlier, neurons typically give rise to spikes with a key feature of its shape being its amplitude or height. Consequently, a relatively simple way to detect

and quantify the spiking activity of a neuron is with a voltage threshold trigger. This threshold detection method is widely used because it offers some obvious advantages, e.g. it requires minimal hardware and software, and often extracts the kind of information experimentalists require. After filtering the raw spiking data, threshold-based algorithms usually detect fluctuations from the baseline signal values by dynamically setting a threshold value. Threshold crossings, in turn, are marked as spiking events (Muthmann et al. [2015], Cyrille Rossant [2016], E. Chung et al. [2017]). However, it is not always possible to accurately separate the desired spikes from the background noise. As a result, in reality the threshold level determines a trade-off between missed spikes (false negatives) and the number of background events that cross the threshold (false positives). Ideally, one would like to set the threshold to optimize the desired ratio of false positives to false negatives. Needless to say, this depends a lot on the quality of the raw spiking data being analysed, i.e. low levels of background noise that are small relative to the spike amplitudes makes this task easier.

2.6.2 Template based strategies:

While approaches based on spike amplitude were one of the earliest and most common spike detection methods, subsequent work reflects the realization that the more features we have, the better our chances of distinguishing different spike shapes. Accordingly, another commonly adopted approach relies on selecting template spike shapes for each recorded event and then assigning the detected spike waveforms through a process called template matching (Gerstein and Clark [1964], Capowski [1976], Millecchia and McIntyre [1978]). However, this method also relies on manual interventions. Previous work involving template matching required the user to choose a small set of spikes, which served as the templates. In this connection, it should be noted that a different approach involves capturing features from the spike shapes that are used for clustering the waveforms. For instance, the peak amplitude and width of the spikes can also be fed as inputs to a clustering algorithm (Lewicki [1998]). In general, a larger array of discriminative features enhances the ability to distinguish the different spike shapes. In general, these template-based algorithms first learn (Pachitariu et al. [2016]) or extract (Prentice et al. [2011]) templates of spike shapes and then scan the raw electrophysiological recording data, to detect events, and eventually assigns them to a particular neuron based on some metric of similarity. The final step of the spike sorting process involves grouping the points in the feature space into clusters, with each cluster associated to a different neuron. An appropriate visualisation framework is then used for subsequent analysis of the sorted spiking events.

2.7 Neural networks applications in spike sorting

As described in the preceding sections, the growing use of high-density multi-electrode array (MEA) recordings in neuroscience has given rise to the challenge of designing more accurate and robust spike sorting algorithms to better analyse massive spike datasets. Despite considerable progress in this area of research, bottlenecks remain in

terms of high computational cost of the algorithms and the time consumed by manual processing. One notable effort in overcoming these computational bottlenecks involved the development of a neural network detection method (known as YASS: Yet Another Spike Sorter; Lee et al. [2017]). Briefly, this neural network based strategy relied on an efficient multistage triage-then-cluster-then-pursuit approach that first focused on only extracting less noisy, high-quality waveforms from the spiking data time series by temporarily avoiding noisy or collided events (i.e. overlapping spikes fired synchronously by two different neurons). This method of efficient outlier triaging entails using the clean waveforms to infer the set of neural spike waveform templates through nonparametric Bayesian clustering. Importantly, this method achieved significant improvements in stability and accuracy on not only biophysically-realistic simulated MEA data, but real spiking data as well. As described in the following sections of this report, the primary goal of the present study is to build and improve upon the above YASS strategy by developing a more efficient and robust neural network detection method for spike sorting.

2.8 Data used in this project

Three datasets have been used in this project. All three were produced by the MEArec library (MEArec [2018]). MEArec is a resource aimed at generating biophysical extracellular neural recordings using Multi-Electrode Arrays (MEA). These recordings combine generation of Extracellular Action Potentials (EAP) templates with spike trains. The recordings are generated by convoluting and modulating EAP templates with spike trains and then adding noise. This effectively allows us to create artificial datasets with varying levels of noise while setting parameters such as minimum distance between neurons, as well as the minimum and maximum amplitude of the templates. The data produced was in the industry-standard HDF5 format. The first dataset used here is a shorter 10 second recording with minimal noise consisting of 320,000 frames. The minimum distance between neurons is set to $15\ \mu\text{m}$ and the minimum amplitude is $10\ \mu\text{V}$. The waveforms produced by these data are clear and comply with the accepted waveform of a spike. This smaller dataset is used to judge the initial performance of the neural network algorithm used for the spike detection tasks in the present study. The second and third datasets are 60-second long recordings with higher levels of noise consisting of 1.92 million frames. Other parameters are kept unchanged. These noisier waveforms exhibited far greater fluctuations and thereby provided a more challenging data set for testing the efficiency of our neural network.

Chapter 3

Methodology

3.1 Pre-processing

Information about the ground-truth datasets are extracted using the `spikeextractors` library(SpikeExtractors [2019]). These data include location of the recorded neurons and the channels - specifically, the timing of the spikes fired by the neurons and the channels the spikes were detected on. The locations of the channels allow us to create a distance matrix that gives us the relative position of each channel from all the other channels. This is crucial because multiple channels may detect the same spike. We use the distance between these channels to distinguish whether two different spikes were detected at the same time.

3.2 Baseline Classifier

The baseline classifier is crucial as it serves as a point of comparison for our results. The baseline classifier used in this project was provided by Cole Hurwitz (Research Postgraduate Student at the Institute for Adaptive and Neural Computation, University of Edinburgh). The classifier is essentially a threshold classifier. It reads snippets of data and records any event that crosses the threshold; this threshold can be adjusted manually. Two more factors are taken into consideration before an event crossing the threshold is classified as a spike (a) the refractory period, and (b) duplicate radius.

(a) The refractory period in this case is the number of frames after a detection, and before a new detection can be registered. This reflects the period of time after a spike has been fired when it is impossible for the neuron to generate another action potential (Figure 2.2).

(b) The duplicate radius is the distance (in microns) between channels for detected spikes to be considered duplicate detections with close detection times.

These are also both manually adjustable. After experimenting, the threshold is set to an optimal value of $38\mu\text{V}$. The refractory period is 10 frames and the duplicate radius

is $100\ \mu\text{m}$ for the studies described below.

3.3 Creating the neural network

I decided to train a simple Multi-Layer Perceptron (MLP) that acts as a binary classifier. Given a 50 frame snippet of voltage data, the model will output 1 if it has detected a spike, or a 0 if it has not. I use the `MLPClassifier` module from the `scikit-learn` library (Pedregosa et al. [2011]). The model uses a Low-memory Broyden-Fletcher-Goldfarb-Shanno (lbfgs) solver, an alpha value of $1\text{e-}5$ and two hidden layers of 5 and 2 neurons respectively. All other parameters remain at their default values ('relu' activation function for the hidden layers with a constant learning rate and 200 maximum iterations). The number of layers and neurons is set to a low value to judge how the model takes to the task with low complexity.

3.4 Creating the training set

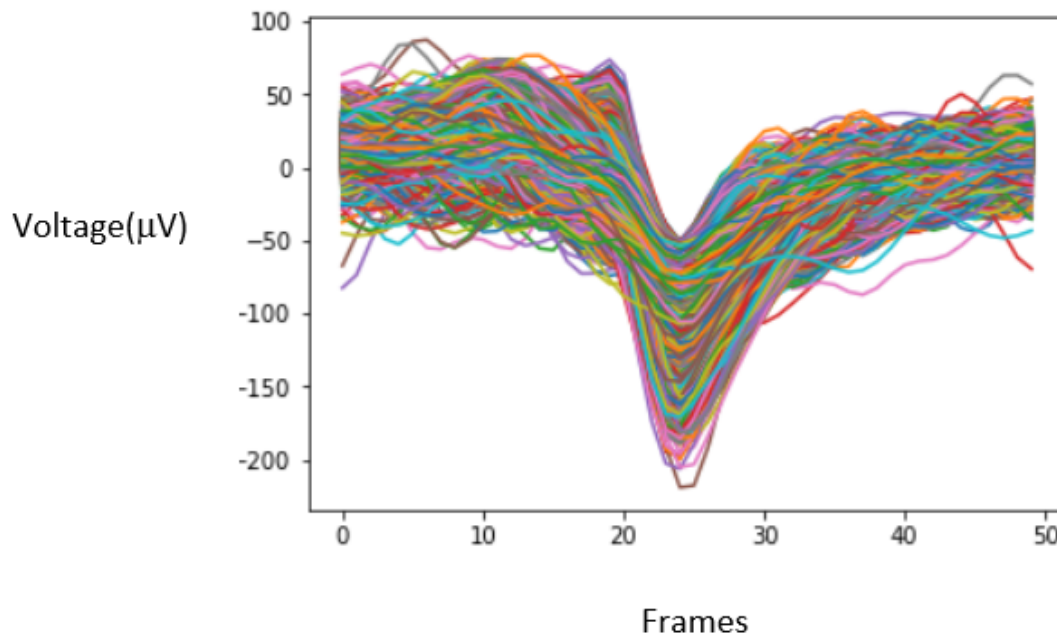


Figure 3.1: Waveforms of confirmed spikes in the training data from a low-noise dataset. Spikes are depicted as negative deflections, wherein the waveforms are plotted as changes in voltage (μV) as a function of the number of frames (0-50).

The first step in is to train a basic Multi-Layer Perceptron (MLP) to detect spikes from a training set. The data is in the format of a time series with voltage on the ordinate or y-axis. The goal is to train the model to learn the waveform of a confirmed spike. To this end, the model is trained on snippets of data that are 50 frames long and include a

spike that is centred along the middle of the snippet and has an amplitude greater than $50\ \mu\text{V}$ (Figure 3.1). 80% of the training data contains confirmed spikes and 20% is made up of random snippets that do not include any spikes. The model outputs either a 1 or 0 indicating whether or not a test snippet of data includes a spike.

3.5 Creating the testing set

Since the model is trained on a series of spikes that are centred along the middle of the x-axis depicting frame numbers (0-50), we ensured that the testing data also conformed to the same format. Thus, the testing data had to be transformed accordingly. However, in the case of testing data we do not have prior knowledge of the location of the spike along the x-axis that represents the frame numbers. Hence, I proposed to overcome this problem by adopting a solution for both centring the data and acquiring higher quality snippets for testing. These are described below.

3.5.1 Centring data around local minimum

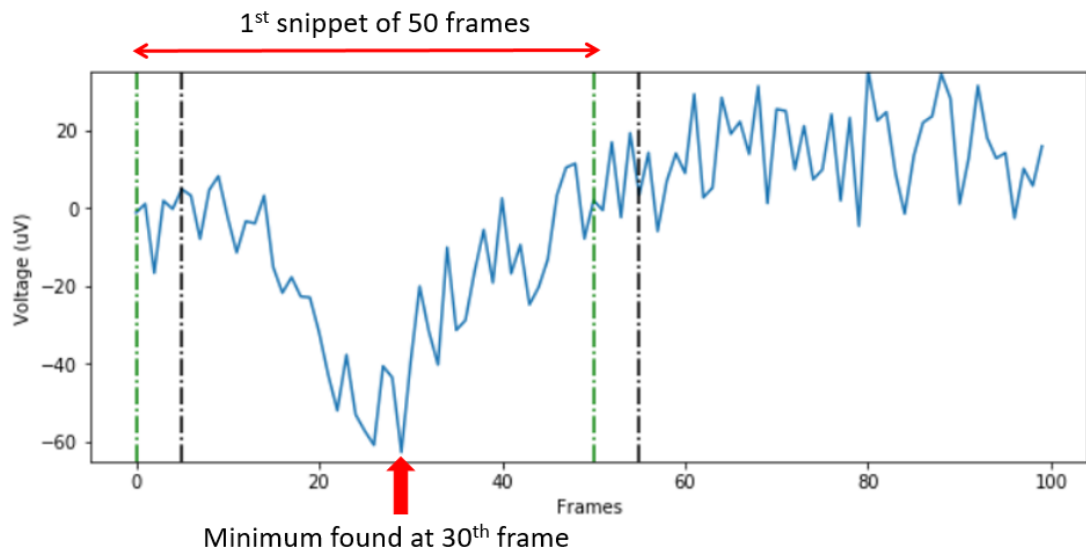


Figure 3.2: Step 1: Search for the first minimum in the first 50 frames(region within green lines). Upon finding the minimum, create a new snippet centred around that point and add it to the test set (region within black lines).

As described earlier, the waveform data is read 50 frames at a time. First, the minimum value of the voltage within this frame is located and is now made the new centre for the data. This in turn means that if there is a spike in this snippet it, by definition, is aligned along this central point of the snippet. This is because the extracellular spike waveforms are represented as negative deflections and thus, the peak of the spike will automatically be the lowest or minimum value along the y-axis representing the voltage amplitudes.

Next, we shift forward by 30 frames from the new centre and search again for the next minimum point and then repeat the process as described above. This process is helpful as it provides a series of snippets containing a segment of data with high negative values of amplitudes, thereby allowing us to check for a spike along many points in that data. At the same time, it ensures that if there is indeed a spike present in any given snippet, that it is centred. This iterative process is demonstrated in the figures below.

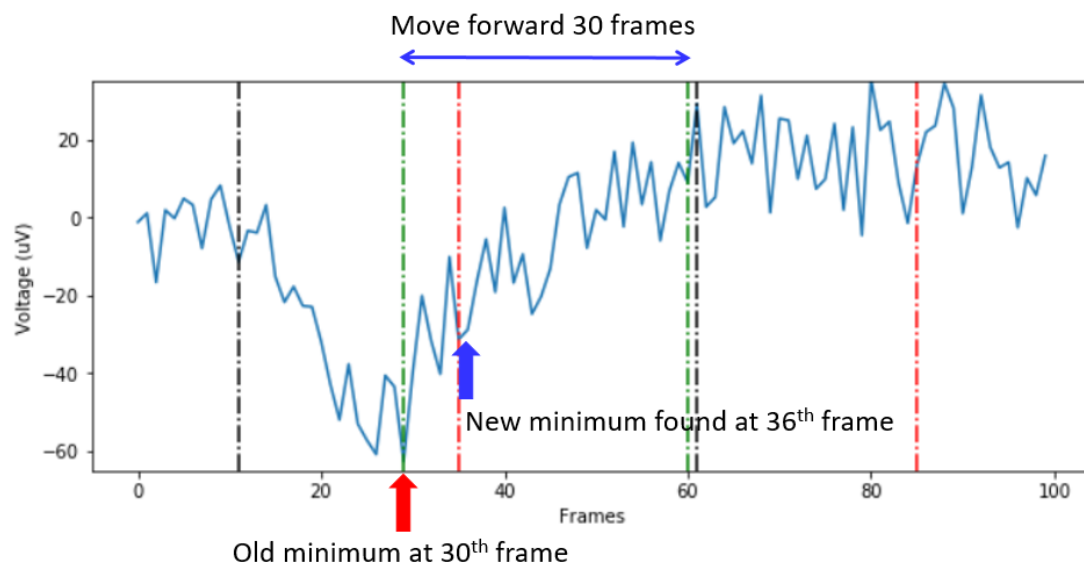


Figure 3.3: Step 2: Start next segmentation at the minimum point located at 30th frame and then move forward by 30 frames and find next minimum in a 50 frame range (region within red lines). This becomes the centre for the second snippet and it is added to the test set (region within black lines).

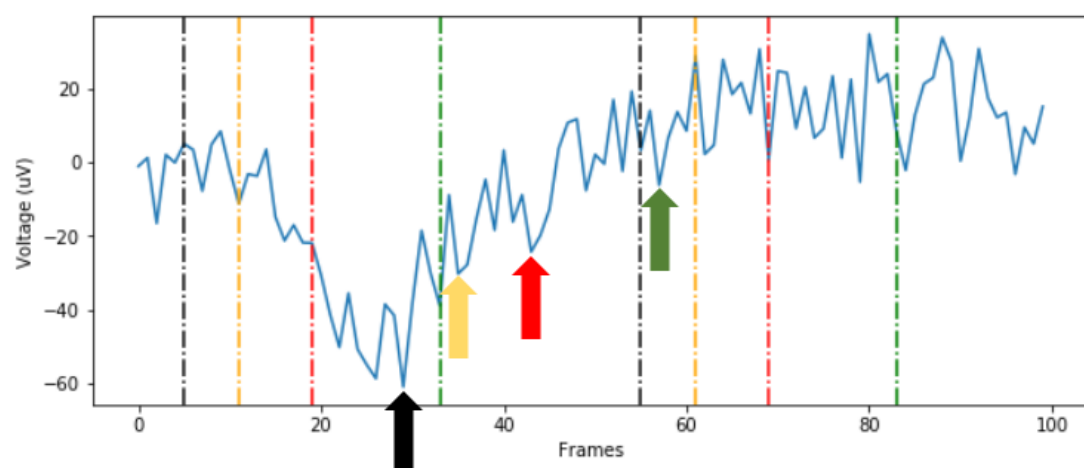


Figure 3.4: Step 3: Repeat this process. The final result is the 4 snippets displayed above. The boundaries for each snippet are marked by identically coloured lines. The minimum of each snippet is marked with an identically coloured arrow.

3.6 Evaluation of model predictions

The MLP classifier outputs either 0 or 1 on each snippet of data. Snippets are read channel-by-channel. I created an evaluation method to produce a final output array of firing times and detected channels. For each event that the model predicts to be a spike, we check our list of detected spikes to see if we already have a spike within 15 frames of the current spike. If there is a match we check the distance of the channel of the current spike to the channel of the previously detected spike. If the distance is greater than $100\text{ }\mu\text{m}$, we consider this to be a new spike fired by a different neuron. On the other hand, if the channels were within $100\text{ }\mu\text{m}$, the spikes were considered to be from the same neuron, but just being detected on different channels that are close to each other. The final product from these analyses is an array of predicted spike times and the channel on which the spike produced the greatest amplitude in terms of voltage.

The final stage of evaluation involves comparisons to the ground-truth confirmed spikes. A jitter time of 10 frames is used for this purpose. If a detected spike is within 10 frames of an actual spike and also on the same channel, it is considered to be a true positive. Further, false positives and false negatives are calculated. Detected spikes from the baseline classifier are evaluated similarly.

Chapter 4

Results

4.1 Spike detection and sorting on low-noise dataset

A basic Multi-Layer Perceptron (MLP) consisting of two hidden layers, the first with 5 neurons and the second with 2, is trained using processed data (explained in section 3.1). The model is trained and tested on different datasets. It is safer to do this as splitting a single dataset may affect the results due to correlation in the waveforms. This is done to see the initial effect of training a neural network on the data. The results thus produced are encouraging. We compare the results to a baseline classifier that uses a threshold. Any event below a certain threshold is classified as a spike in the classifier. For a clean dataset this is a fairly effective baseline because with optimization it produces high accuracy, as summarized in Table 4.1.

While there is a slight reduction in total accuracy, there is also a notable decrease in the number of false negatives. To gain a better understanding of the overall performance of the neural network we analysed the waveforms of true positives, false positives and false negatives. As expected the waveform of true positives conforms to the expected shape. What is particularly encouraging is the observation that the average shape of false positives is also very good because their shapes matches closely with that of a good spike. The final confirmation of a successful implementation comes from the shape of the false negatives. These do not resemble the shape of a real spike. Based on this information it seems there are discrepancies in the dataset as expected. The ground-truth spikes do not always produce a clear waveform that fully satisfy the criteria for a regular spike. This could be due to collisions between spikes and also due to the distance of the channel from the neuron being too large. A lot of the false positives

	BASELINE	MULTI-LAYER PERCEPTRON
TRUE POSITIVES	3180	2915
FALSE POSITIVES	180	570
FALSE NEGATIVES	191	38
ACCURACY	89.5%	82.7%

Table 4.1: Classification results on the low-noise dataset

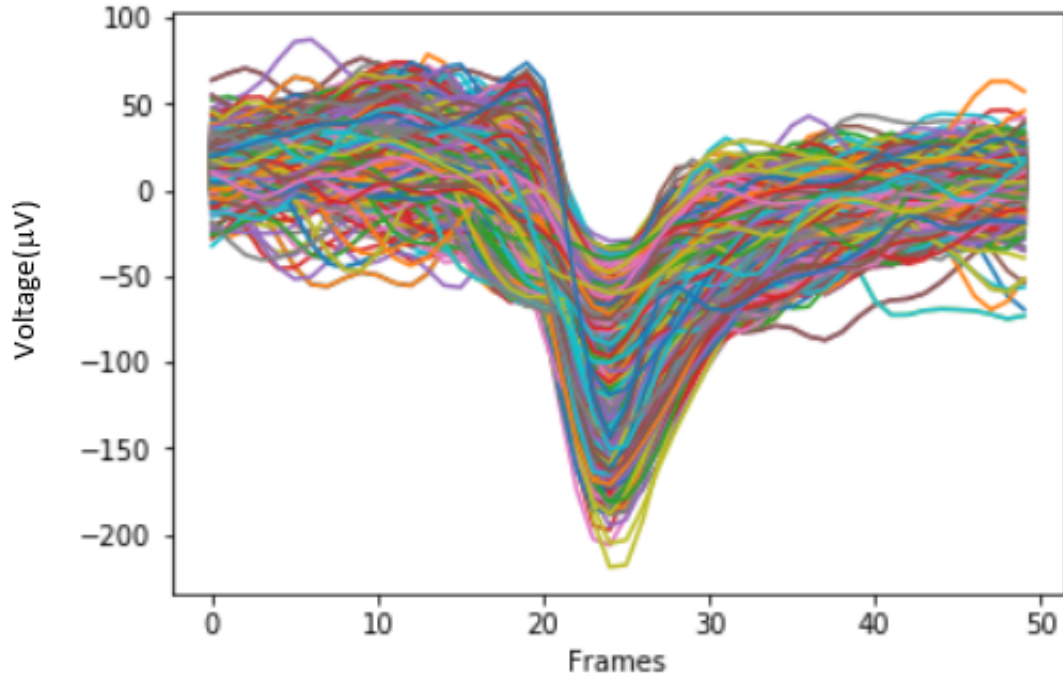


Figure 4.1: Waveform of true positives in low-noise dataset

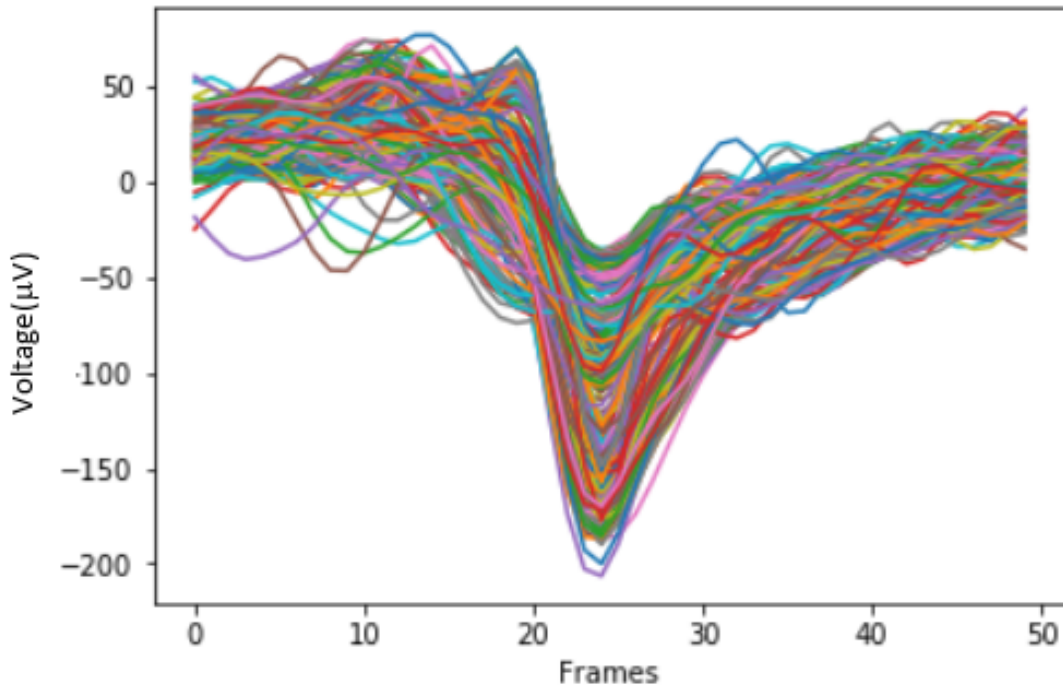


Figure 4.2: Waveform of false positives in low-noise dataset

may be spikes that were detected on the wrong channel. My method assigns a spike to the channel on which it produced the greatest amplitude. However, the ground-truth

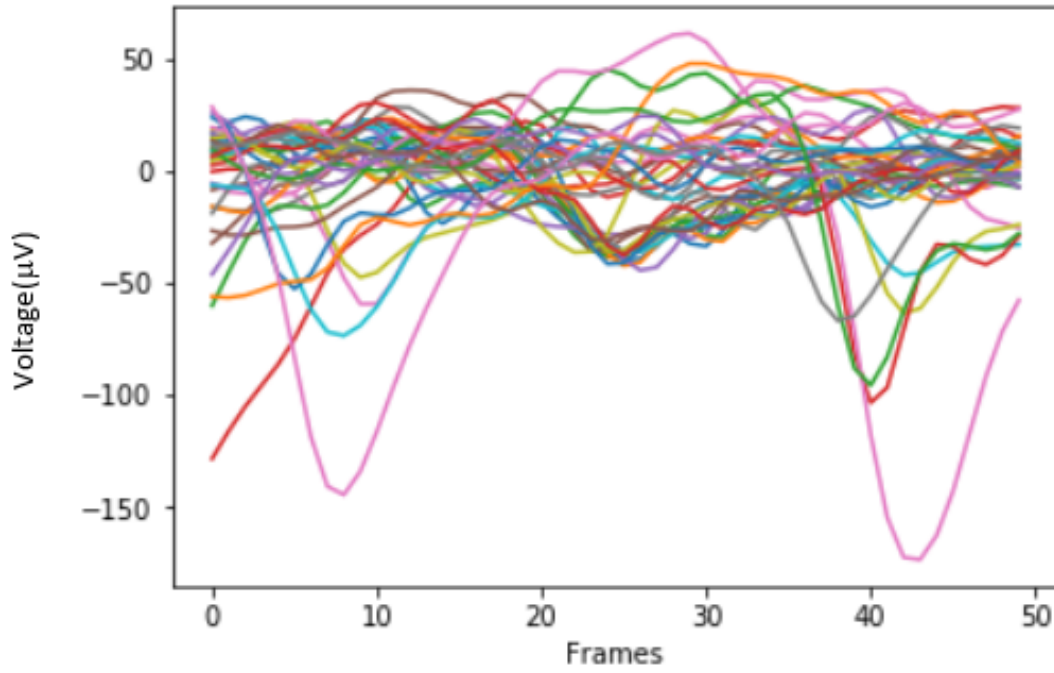


Figure 4.3: Waveform of false negatives in low-noise dataset

does not follow this procedure. This may explain the discrepancy seen here.

4.2 Spike detection and sorting on high-noise dataset

As described above, our MLP method is capable of detecting spikes with high degree of accuracy and efficiency. Having established this methods efficacy using the low-noise dataset, we decided to extend our analysis to a more challenging task apply the same strategy to detect spikes in a high-noise dataset. To this end, we next applied the same procedure on a much larger and noisier dataset. (1,920,000 frames per channel, 100 channels)

	BASELINE	MULTI-LAYER PERCEPTRON
TRUE POSITIVES	20312	20048
FALSE POSITIVES	34647	15960
FALSE NEGATIVES	409	673
ACCURACY	36.6%	54.6%

Table 4.2: Classification results on the low-noise dataset

Not surprisingly, the same model now achieves a significantly lower accuracy on the noisier dataset. Despite this, it still outperforms the baseline classifier. We probed this further by carrying out a more detailed analysis of the false positives and false negatives. This reveals the reasons for the lower levels of accuracy with the high-noise

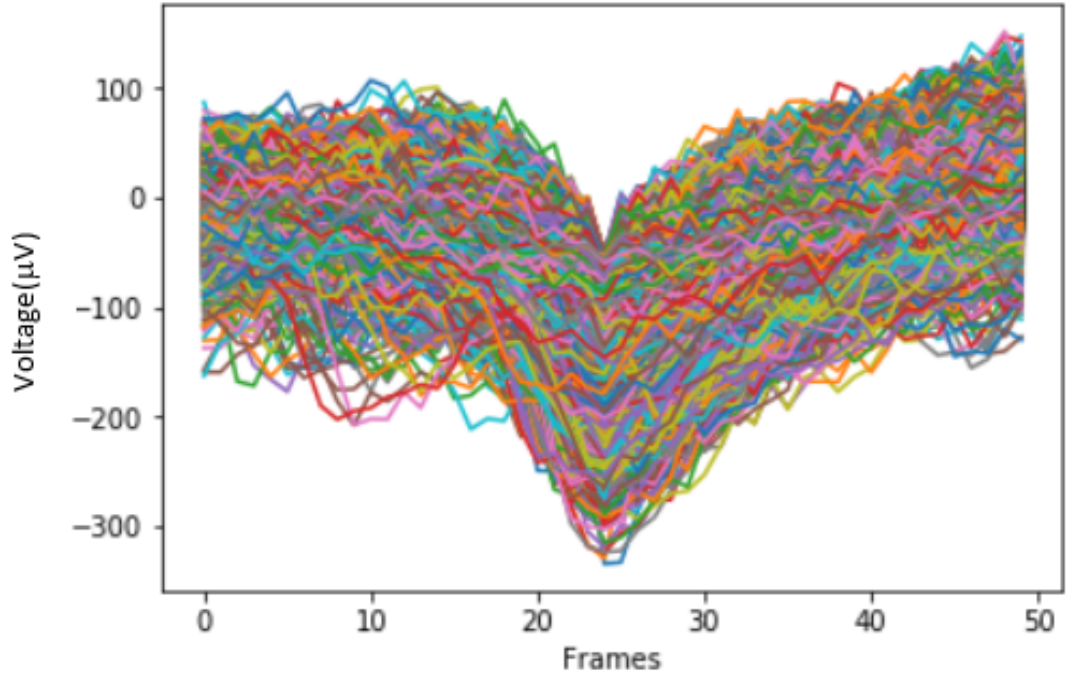


Figure 4.4: Waveform of spikes in training set from high-noise dataset

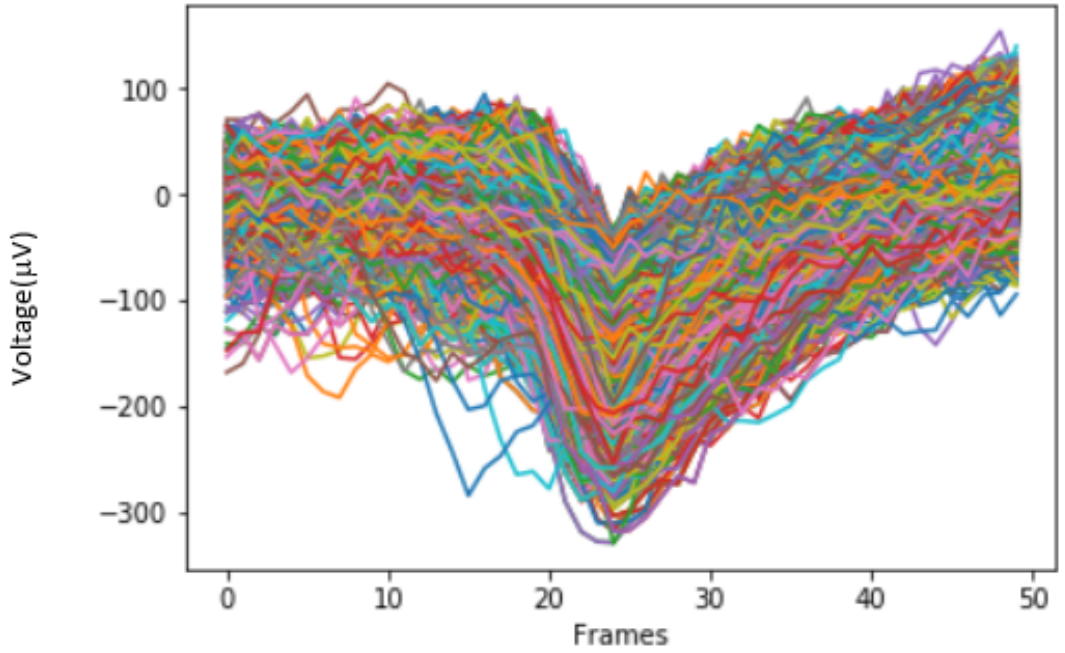


Figure 4.5: Waveform of false positives in high-noise dataset

dataset. First, the false positives have a waveform shape that conforms to the training set, indicating that the spike detection aspect of the model is fairly effective despite the higher noise. In contrast, the false negative waveforms do not in any way reflect

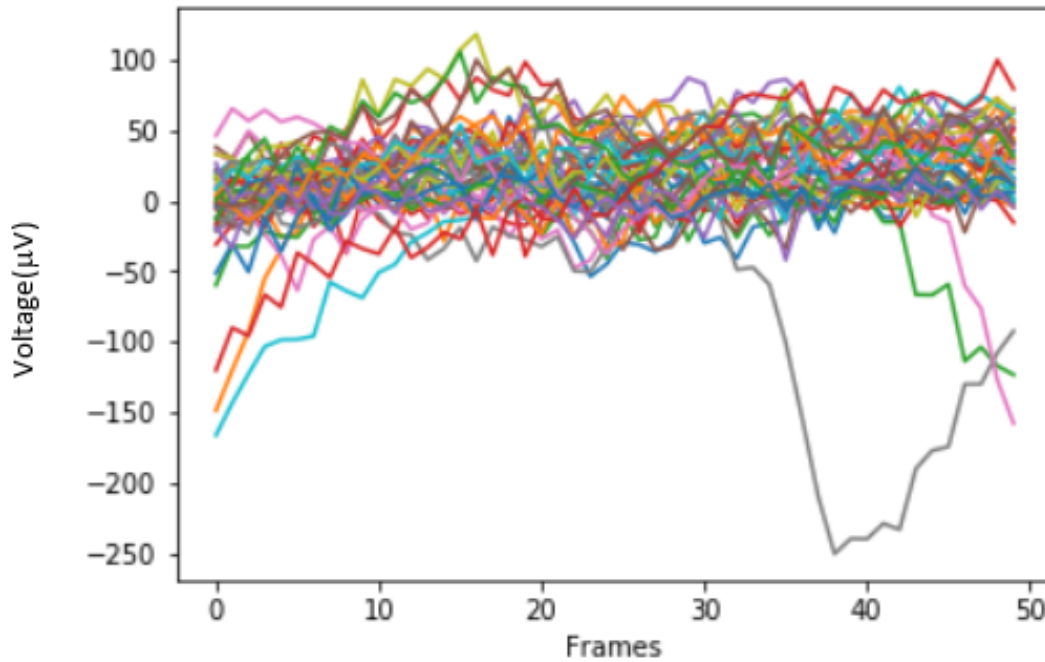


Figure 4.6: Waveform of false negatives in high-noise dataset

the shape of a real spike. This raises the possibility that a significant proportion of the ground-truth spikes do not reliably reflect the change in voltage that should accompany the firing of an actual action potential. These problems usually arise due to collisions, i.e. multiple spikes firing at the same time thereby making it more difficult to assign them to specific neurons. In other words, although our model succeeds in detecting spikes even in a noisy dataset, it is the spike sorting aspect, i.e. assigning them to the right neuron, wherein the model is performing poorly. Once a spike is detected it needs to be attributed to a channel. My model attributes it to the channel that detects a waveform with the highest amplitude. This is likely the reason for many false positives as intermediary channels pick up a combined voltage from multiple neurons around, thereby producing a high voltage value which gives the false appearance of a spike.

4.3 Effect of snippet length on model performance

One of the outcomes of the procedure being used to create the testing dataset is the introduction of a new parameter - snippet length. Thus far I have used snippets of data that are 50 frames long. This raises the question - what is the effect of increasing the size of the snippets? This will likely reduce the runtime of the program when it comes to creating the dataset as we analyse larger chunks of data at a time. If the model performs fairly well then increasing the snippet length could be beneficial in terms of efficiency. I decided to try out snippets of 70 frames. The model is both trained and tested on snippets of 70 frames with the data still centred along the minimum. Results obtained from this on the high-noise dataset are summarised in Table 4.3.

	50 SNIPPET MODEL	70 SNIPPET MODEL
TRUE POSITIVES	20048	20125
FALSE POSITIVES	15960	19505
FALSE NEGATIVES	673	596
ACCURACY	54.6%	50.0%

Table 4.3: Classification results of 50 and 70 snippet models on the high-noise dataset

The model shows a slight reduction in performance (approx. 4%). However, the program takes 28% less time to run. Hence, there appears to be a fair trade-off in terms of speed and accuracy. The model predicts a larger number of false positives when the snippet length is increased. This might be because larger snippets are more likely to have other high amplitude events since there are now 35 frames of data on either side of the minimum as opposed to 25 frames previously. An increase in high amplitude events is likely to sway the model into detecting more spikes. This suggests shorter snippet lengths despite being computationally inferior are likely to have better accuracy.

4.4 Adding neurons and a hidden layer to the model

We have seen how the model performs with 2 small hidden layers. We now conduct an experiment to see how the results translate to a more complex system. A third hidden layer was added to the model and the number of neurons in the hidden layers was increased. Specifically, to 25 neurons in the first layer, 10 neurons in the second layer and 5 neurons in the third layer. These values were chosen as previous research suggests (Heaton [2017]) that the number of neurons should gradually move from the number of input variables towards the number of output variables (50 to 1 in this case). The results obtained from this experiment are summarized in Table 4.4.

	ORIGINAL MLP	NEW MLP
TRUE POSITIVES	20048	20193
FALSE POSITIVES	15960	42270
FALSE NEGATIVES	673	528
ACCURACY	54.6%	32.1%

Table 4.4: Classification results of old MLP with 2 hidden layers and new MLP with 3 hidden layers on the high-noise dataset

These results show that performance has dropped considerably, as evidenced by a 18% reduction in accuracy. Further, the number of false positives has more than doubled, while there was only a marginal decrease in false negatives. This suggests the model was somewhat indiscriminate when it came to predicting whether a snippet had a spike in it. Closer analysis of the training method and model reveal why this may be the case. In Section 3.4 we discussed how the training set for the model was created. 80% of the training points consisted of confirmed spike waveforms with an output of 1. Only 20% of the training points would output a 0. In this connection, it may be noted that (Wei

and Dunbrack [2013]) showed that using balanced training data (50% positives and 50% negatives) results in the highest balanced accuracy (the average of True Positive Rate and True Negative Rate). In their work on bioinformatics data, binary classifiers performed the best when trained on balanced datasets. Therefore, it seems the more complex model learnt to detect spikes more often, because 80% of the data it was trained on contained spikes.

4.5 Asymmetric snippets

All experiments conducted till this point have had spikes in the training set centred around the 25th frame (centre of snippet) and testing snippets centred around minimum points. We now try an approach where the training spikes and minimum of the testing snippets is aligned along the 15th frame. Significant voltage information is often contained in the time right after a spike. By aligning along the 15th frame we increase the scope of post spike voltage in our data. Results are shown in Table 4.5.

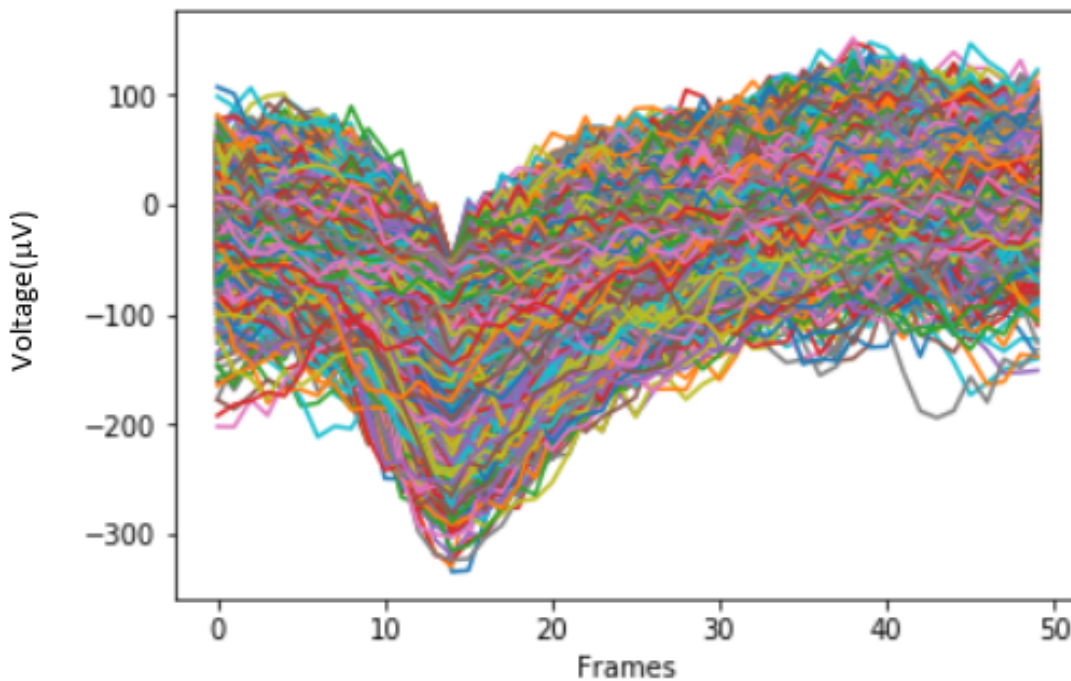


Figure 4.7: Waveform of asymmetric training set from high-noise dataset

We observe a 7.5% decrease in performance. Reasons for this may be similar to the reason for decline in performance observed in Section 4.3. By aligning the data on the 15th frame, we now have 35 frames of data after our point of interest (the minimum). This gives 10 more frames after the minimum for another high amplitude event to occur. The further we move away from the spike, the higher the probability of another high amplitude event as we start crossing the refractory period. As mentioned

	ORIGINAL MLP	ASYMMETRIC MLP
TRUE POSITIVES	20048	20091
FALSE POSITIVES	15960	21896
FALSE NEGATIVES	673	630
ACCURACY	54.6%	47.1%

Table 4.5: Classification results of original symmetric MLP and asymmetric MLP

in Section 4.3, more high amplitude events will likely sway the model into detecting more false spikes.

Chapter 5

Discussion

Action potentials constitute a vital component of neural communication. Consequently, elucidating the neural code embedded in the spatio-temporal patterns of spiking has been a key focus of both experimental and computational neuroscience. Over the years, this line of research has relied heavily on electrophysiological recordings using a range of in vitro and in vivo techniques. Recent advances in the fabrication and use of MEAs has greatly increased the power and sophistication of such recording techniques (Hilgen et al. [2017], Stevenson and Kording [2011], J. Jun et al. [2017]). These, in turn, have given rise to huge volumes of spiking data gathered from recordings from large numbers of neurons. Further, these spikes are recorded simultaneously across multiple electrodes, thereby posing a major computational challenge. As a result, there is a growing need for more robust, accurate and scalable methods for spike sorting and analysis to keep pace with the rapid growth of large-scale experimental spiking data.

Early work on the development and implementation of spike sorting strategies relied on methods, such as threshold and template based algorithms (Lewicki [1998], Rey et al. [2015]). However, many of these approaches required manual tuning and, hence, were time consuming and variabilities were introduced by the human factor. Moreover, the rapid growth in the volume of spiking data also highlighted the urgency of developing more automated and efficient methods of spike detection and sorting (Muthmann et al. [2015]).

The present study addresses certain aspects of this bigger problem by testing the efficacy of a neural network detection method to carry out efficient spike detection from biophysically-realistic simulated MEA data containing both low and high levels of background noise.

5.1 Key findings

Some of the earlier spike sorting strategies, such as threshold/amplitude or template spike-shape based detection methods, required varying levels of manual interventions

and readjustments. This added time and human variability, thereby impairing scalability, efficiency and reliability. More recently, strategies using neural network based detection tools, such as YASS, has overcome many of these earlier limitations (Lee et al. [2017]). Findings from the present study reiterate the power and utility of such a strategy. In contrast to conventional spike sorting approaches, this method rapidly learns to detect action potentials present in the signal. First, compared to the more sophisticated convolution based method utilized by YASS, the current study relied on a relatively simple Multi-Layer Perceptron (MLP) consisting of only two hidden layers (with 5 neurons in the first layer, 2 in the second). Despite this, our model yielded high levels of accuracy. Second, this level of accuracy was achieved without requiring any time-consuming manual interventions. Third, this was possible with speed and low computational cost. Together, this model, despite its relative simplicity, succeeds in addressing two of the key challenges faced by many spike detection methods - accuracy and speed. Importantly, the neural network, using the training dataset, was also able to learn the features of the spike waveforms, thereby further increasing its efficiency and utility.

Not surprisingly, the best performance using our model was achieved on the low-noise dataset. This was evident from the high accuracy shown in Table 4.1 and waveforms displayed in Figures 4.1, 4.2 and 4.3. As expected, the higher noise dataset posed significant challenges as evidenced by the reduction in performance. However, in terms of reliable and accurate spike detection, the primary goal of the present study, our model continued to perform well even with the high-noise dataset as shown by the waveforms in Figures 4.5 and 4.6. However, the most notable decrease in performance was seen in the domain of spike sorting, specifically assigning a detected spike to the correct channel. As mentioned earlier, the MLP used here is a rather basic one and has its limitations. Perhaps future performance can be boosted significantly by trying different models like Convolutional Neural Networks used in YASS and by implementing Bayesian Parameter Optimisation techniques.

5.2 Future directions

In conclusion, the present study may further open new ways to build more robust and scalable neural network methods for efficient and accurate detection and sorting of spiking data. An obvious roadmap for further improvement for detecting and sorting spikes from higher noise datasets would include changing some key facets of the MLP used in the present study. These could include balancing the training dataset as described in Section 4.4 . Another potential angle that is worth investigating in the future would involve the inclusion of Bayesian Parameter Optimisation. This motivation comes from the earlier work done by Jano Horvath in Prof. Matthias Hennig's Lab (University of Edinburgh). Incorporation of these methods is likely to overcome some of the shortcomings of the present model, especially in the area of optimal parameter selection for both the spike detection and especially the spike sorting aspects of the project. The use of neural networks introduces a whole set of parameters such as learning rate, number of hidden layers and number of neurons per layer that can be

optimized using these techniques. Section 4.3 and Section 4.5 also introduced snippet length as an additional parameter that can be optimised for future work using this model.

Of course, building on the current results, we will also need to test how our method, trained and tested using realistic simulated MEA data, fares in analysing real spiking data. Finally, looking ahead beyond the traditional focus on quantification of sorting accuracy in terms of false positives and missed spikes, this line of work will have to take into account the growing importance of other measures being used in experimental neuroscience, such as spike synchrony (Pazienti and Grün [2006]), and rate code estimates (Ventura [2009]).

Through my work on this project, I have come to appreciate one of the most striking aspects about spike sorting methods - there is no clear consensus about spike sorting standards despite decades of research in this field. In this context, it is particularly interesting to note that future breakthroughs and new insights in this field are increasingly likely to come through a combination of technological advances in MEA recordings and the application of neural network methods to analyse the large-scale data gathered from such techniques. Perhaps there is a tinge of irony in all of this because an artificial neural network, at best, captures only a few major features of how the brain learns to recognise important patterns from the noisy real world. And now these same artificial neural networks may help us decode the meaning of neural activity in the real nervous system.

Bibliography

- Joseph J. Capowski. Characteristics of neuroscience computer graphics displays and a proposed system to generate those displays. *SIGGRAPH Comput. Graph.*, 10(2):257–261, July 1976. ISSN 0097-8930. doi: 10.1145/965143.563319. URL <http://doi.acm.org/10.1145/965143.563319>.
- R. Chandra and L. M. Optican. Detection, classification, and superposition resolution of action potentials in multiunit single-channel recordings by an on-line real-time neural network. *IEEE Transactions on Biomedical Engineering*, 44(5):403–412, May 1997. ISSN 0018-9294. doi: 10.1109/10.568916.
- Dan FM Goodman John Schulman Maximilian LD Hunter Aman B Saleem Andres Grosmark Mariano Belluscio George H Denfield Alexander S Ecker Cyrille Rossant, Shabnam N Kadir. Spike sorting for large, dense electrode arrays. *Nature Neuroscience*, 19:634–641, 2016.
- Jason E. Chung, Jeremy F. Magland, Alex H. Barnett, Vanessa Tolosa, Angela C. Tooker, Kye Y. Lee, Kedar Shah, Sarah H. Felix, Loren Frank, and Leslie F. Greengard. A fully automated approach to spike sorting. *Neuron*, 95:1381–1394.e6, 09 2017. doi: 10.1016/j.neuron.2017.08.030.
- G. L. Gerstein and W. A. Clark. Simultaneous studies of firing patterns in several neurons. *Science*, 143(3612):1325–1327, 1964. ISSN 0036-8075. doi: 10.1126/science.143.3612.1325. URL <http://science.sciencemag.org/content/143/3612/1325>.
- Jeff Heaton, 2017. URL <https://www.heatonresearch.com/2017/06/01/hidden-layers.html>.
- Gerrit Hilgen, Martino Sorbaro, Sahar Pirmoradian, Jens-Oliver Muthmann, Ibolya Edit Kepiro, Simona Ullo, Cesar Juarez Ramirez, Albert Puente Encinas, Alessandro Maccione, Luca Berdondini, Vittorio Murino, Diego Sona, Francesca Cella Zancchi, Evelyn Sernagor, and Matthias Helge Hennig. Unsupervised spike sorting for large-scale, high-density multielectrode arrays. *Cell Reports*, 18(10):2521 – 2532, 2017. ISSN 2211-1247. doi: <https://doi.org/10.1016/j.celrep.2017.02.038>. URL <http://www.sciencedirect.com/science/article/pii/S221112471730236X>.
- A. L. Hodgkin and A. F. Huxley. Currents carried by sodium and potassium ions through the membrane of the giant axon of loligo. *The Journal of Physiology*, 116

- (4):449–472, 1952. doi: 10.1113/jphysiol.1952.sp004717. URL <https://physoc.onlinelibrary.wiley.com/doi/abs/10.1113/jphysiol.1952.sp004717>.
- James J. Jun, Nick Steinmetz, Joshua H. Siegle, Daniel J. Denman, Marius Bauza, Brian Barbarits, Albert K. Lee, Costas Anastassiou, Alexandru Andrei, Cagatay Aydin, Mladen Barbic, Tim Blanche, Vincent Bonin, Joao Couto, Barundeb Dutta, Sergey Gratiy, Diego Gutnisky, Michael Husser, Bill Karsh, and Timothy D. Harris. Fully integrated silicon probes for high-density recording of neural activity. *Nature*, 551:232–236, 11 2017. doi: 10.1038/nature24636.
- B.H. Jansen. Artificial neural nets for k-complex detection. *IEEE engineering in medicine and biology magazine : the quarterly magazine of the Engineering in Medicine and Biology Society*, 9:50–2, 02 1990. doi: 10.1109/51.59213.
- JinHyung Lee, David Carlson, Hooshmand Shokri, Weichi Yao, Georges Goetz, Espen Hagen, Eleanor Batty, EJ Chichilnisky, Gaute Einevoll, and Liam Paninski. Yass: Yet another spike sorter. *bioRxiv*, 2017. doi: 10.1101/151928. URL <https://www.biorxiv.org/content/early/2017/06/19/151928>.
- Michael S Lewicki. A review of methods for spike sorting: the detection and classification of neural action potentials. *Network: Computation in Neural Systems*, 9(4):R53–R78, 1998. doi: 10.1088/0954-898X\9\4_001. URL https://doi.org/10.1088/0954-898X_9_4_001. PMID: 10221571.
- MEArec, 2018. URL <https://github.com/alejoe91/MEArec>.
- Ronald Millecchia and Thomas McIntyre. Automatic nerve impulse identification and separation. *Computers and Biomedical Research*, 11(5):459 – 468, 1978. ISSN 0010-4809. doi: [https://doi.org/10.1016/0010-4809\(78\)90003-4](https://doi.org/10.1016/0010-4809(78)90003-4). URL <http://www.sciencedirect.com/science/article/pii/0010480978900034>.
- Jens-Oliver Muthmann, Hayder Amin, Evelyne Sernagor, Alessandro Maccione, Dagmara Panas, Luca Berdondini, Upinder S. Bhalla, and Matthias H. Hennig. Spike detection for large neural populations using high density multielectrode arrays. *Frontiers in Neuroinformatics*, 9:28, 2015. ISSN 1662-5196. doi: 10.3389/fninf.2015.00028. URL <https://www.frontiersin.org/article/10.3389/fninf.2015.00028>.
- Martin A. R. Fuchs P. A. Brown D. A. Diamond M. E. Nicholls, J. G. and D. A. Weisblat. *From neuron to brain*. Sinauer Associates, fifth edition, 2011.
- Marius Pachitariu, Nicholas Steinmetz, Shabnam Kadir, Matteo Carandini, and Harris Kenneth D. Kilosort: realtime spike-sorting for extracellular electrophysiology with hundreds of channels. *bioRxiv*, 2016. doi: 10.1101/061481. URL <https://www.biorxiv.org/content/early/2016/06/30/061481>.
- Antonio Paziienti and Sonja Grün. Robustness of the significance of spike synchrony with respect to sorting errors. *Journal of Computational Neuroscience*, 21(3):329–342, Dec 2006. ISSN 1573-6873. doi: 10.1007/s10827-006-8899-7. URL <https://doi.org/10.1007/s10827-006-8899-7>.

- F. Pedregosa, G. Varoquaux, A. Gramfort, V. Michel, B. Thirion, O. Grisel, M. Blondel, P. Prettenhofer, R. Weiss, V. Dubourg, J. Vanderplas, A. Passos, D. Cournapeau, M. Brucher, M. Perrot, and E. Duchesnay. Scikit-learn: Machine learning in Python. *Journal of Machine Learning Research*, 12:2825–2830, 2011.
- PhysiologyWeb, 2019. URL <https://www.physiologyweb.com/>.
- Jason S. Prentice, Jan Homann, Kristina D. Simmons, Gaper Tkaik, Vijay Balasubramanian, and Philip C. Nelson. Fast, scalable, bayesian spike identification for multi-electrode arrays. *PLOS ONE*, 6(7):1–12, 07 2011. doi: 10.1371/journal.pone.0019884. URL <https://doi.org/10.1371/journal.pone.0019884>.
- Hernan Gonzalo Rey, Carlos Pedreira, and Rodrigo Quian Quiroga. Past, present and future of spike sorting techniques. *Brain Research Bulletin*, 119:106 – 117, 2015. ISSN 0361-9230. doi: <https://doi.org/10.1016/j.brainresbull.2015.04.007>. URL <http://www.sciencedirect.com/science/article/pii/S0361923015000684>. Advances in electrophysiological data analysis.
- SpikeExtractors, 2019. URL <https://github.com/SpikeInterface/spikeextractors>.
- Ian H. Stevenson and Konrad Paul Kording. How advances in neural recording affect data analysis. *Nature Neuroscience*, 14(2):139–142, 2 2011. ISSN 1097-6256. doi: 10.1038/nn.2731.
- Valérie Ventura. Traditional waveform based spike sorting yields biased rate code estimates. *Proceedings of the National Academy of Sciences*, 106(17):6921–6926, 2009. ISSN 0027-8424. doi: 10.1073/pnas.0901771106. URL <https://www.pnas.org/content/106/17/6921>.
- Qiong Wei and Roland L. Dunbrack, Jr. The role of balanced training and testing data sets for binary classifiers in bioinformatics. *PLOS ONE*, 8(7):1–12, 07 2013. doi: 10.1371/journal.pone.0067863. URL <https://doi.org/10.1371/journal.pone.0067863>.